



Dual-band, Dynamically Tunable Plasmonic Metamaterial Absorbers Based on Graphene for Terahertz Frequencies

S. Jarchi^{*a}, J. Rashed-Mohassel^b, M. Mehranpour^a

^a Faculty of Technical and Engineering, Imam Khomeini International University (IKIU), Qazvin, Iran

^b School of Electrical & Computer Engineering, College of Engineering, University of Tehran, Tehran, Iran

PAPER INFO

Paper history:

Received 23 May 2018

Received in revised form 19 January 2019

Accepted 07 March 2019

Keywords:

Graphene

Metamaterial

Terahertz Absorber

Tunable Absorber

Dual-band Absorber

ABSTRACT

In this paper, a compact plasmonic metamaterial absorber for terahertz frequencies is proposed and simulated. The absorber is based on metamaterial graphene structures, and benefits from dynamically controllable properties of graphene. Through patterning graphene layers, plasmonic resonances are tailored to provide a dual band as well as an improved bandwidth absorption. Unit cell of the designed structure is made of four complementary square rings, on a thin grounded SiO₂ layer of 5 μm thickness. Four splits are included in the square rings to provide continuity of graphene layer. Dual band absorption of 90% is provided, which frequency of peak absorption increases with increasing chemical potential of graphene layer. It is shown that with varying dimensions of the split rings an improved bandwidth absorber is also achieved, where absorption band increases with increasing graphene's chemical potential either. To better understand excitation of plasmonic resonances on the proposed structure, electric field distribution on the graphene layer as well as at the unit cell's cross section is investigated and graphically demonstrated. Dependence of absorption on incidence and polarization angles of the incoming wave is studied and also graphically presented.

doi: 10.5829/ije.2019.32.4a.07

1. INTRODUCTION

Metamaterial structures have been extensively applied in microwave frequency bands for providing enhancement in active and passive devices. Metamaterials have been applied to design and improve microwave devices such as transmission lines, antennas, absorbers, etc. [1-5]. After their realization and successful applications in microwave frequencies, tremendous efforts raised to take advantage of their extraordinary features in terahertz and optical frequencies. Terahertz absorbers using metamaterials have been developed due to their wide range of employments in terahertz detectors, sensors, stealth applications and so forth. Recently graphene, one layer of carbon atoms in hexagonal lattice, has received special interest in terahertz and optical frequencies due to its beneficial effects specifically its dynamically tunable property.

A vast amount of researches include the design of metamaterial terahertz absorbers based on either metal or

graphene sheets. A four band and polarization insensitive metamaterial absorber is proposed in literature [6]. In this structure gold is used as metal and a relatively thick substrate with 16 μm thickness is applied. A broadband and polarization insensitive terahertz absorber, as well as a metamaterial based perfect absorber using multilayer metamaterial structures, both using gold as metal, are designed in literature [7, 8] respectively. However fabrication of multilayer structures is complicated and challenging. A broadband terahertz absorber and a perfect metamaterial absorber on a single dielectric layer are designed in literature [9, 10], respectively. In these absorbers gold is employed for patterned metallic layer and unit cell's lateral dimensions equal 0.33 and 0.27 wavelengths at the lowest absorption frequency, respectively; which are relatively high. Several complementary planar metamaterials, using gold, on a thick dielectric with 625 μm thickness, are proposed in literature [11].

*Corresponding Author Email: s.jarchi@eng.ikiu.ac.ir (S. Jarchi)

From metamaterial absorber designs using graphene we can refer to literature [12], where a free standing monolayer metamaterial graphene sheet is investigated and 50% absorption is achieved. A perfect metamaterial absorber made of graphene ribbons is proposed in literature [13]. Ultra-wideband metamaterial graphene ribbons on a thick dielectric with 118 μm thickness, and a tunable graphene based metamaterial absorber on a relatively thick dielectric with 17 μm thickness, are proposed in literature [14, 15], respectively. A broadband tunable terahertz metamaterial absorber based on graphene, is designed in literature [16]. In this structure, with varying graphene's chemical potential broadband performance changes to a narrowband absorber, albeit there isn't a direct relation between absorption frequency and graphene's chemical potential.

Literature survey of metamaterial terahertz absorbers reveals that applying graphene instead of metals results in absorbers with smaller unit cell dimensions and tunable properties. In this paper a dual-band with improved bandwidth tunable metamaterial terahertz absorber based on graphene, with identical unit cell dimensions and similar configurations, on a 5 μm grounded SiO_2 substrate is designed and investigated. The designed structure are dynamically controllable with increasing graphene's chemical potential, through applying a static biasing voltage. The absorbers are thin and compact. Simulations are performed using CST microwave studio.

2. THEORY OF THE DESIGN

The proposed tunable absorber is designed based on graphene. Graphene is a mono-layer of carbon atoms in hexagonal lattice. It is shown that graphene in low terahertz frequencies can support plasmonic excitations, both propagating and localized [17]. Graphene is modeled numerically using a sheet with surface conductivity σ_{gr} . Its conductivity is affected by inter-band and intra-band contributions [15]:

$$\sigma_s = \sigma_s^{intra} + \sigma_s^{inter} \quad (1)$$

$$\sigma_s^{intra} = \frac{2k_B T e^2}{\pi \hbar^2} \ln \left(2 \cosh \frac{E_f}{2k_B T} \right) \frac{i}{\omega + i\tau^{-1}} \quad (2)$$

$$\sigma_s^{inter} = \frac{e^2}{4\pi \hbar} \left[H \left(\frac{\omega}{2} \right) + i \frac{4\omega}{\pi} \int_0^\infty \frac{H(\Omega) - H(\omega/2)}{\omega^2 - 4\Omega^2} d\Omega \right] \quad (3)$$

where T is temperature in Kelvin; $2\Gamma = \hbar/\tau$ and τ is electron-phonon relaxation time; e , \hbar and k_B are constants and denote electron charge, Planck's and Boltzmann's constants respectively; E_f is Fermi energy and can be tuned by applying a static bias voltage [13].

In low Terahertz regime, only the intra-band contribution is considerable and is required to be taken into account. Furthermore for $E_f \gg K_B T$ the intra-band

term, with reasonable accuracy, can be simplified according to literature [15]:

$$\sigma_s \approx \frac{e^2 E_f}{\pi \hbar^2} \frac{i}{\omega + i\tau^{-1}} \quad (4)$$

Which represents a Drude like property with linear dependency of conductivity on Fermi energy. Thus with varying graphene's Fermi energy or chemical potential, surface conductivity is dynamically tunable.

As mentioned, graphene in low Terahertz regime has similar properties to metals with the advantage of being tunable with varying chemical potential through applying electrostatic voltage. Interaction of an incident wave with the graphene sheet occurs through excitation of plasmonic resonances. By patterning graphene sheet, surface conductivity is modified and can be tailored to provide plasmonic resonances at desired frequencies. In order to investigate effective surface conductivity of patterned graphene sheet, numerical methods are proposed in literature [15,18]. In this method graphene's surface conductivity is investigated from reflection and transmission coefficients of the structure or the ABCD matrix.

3. METAMATERIAL STRUCTURE DESIGN

The designed metamaterial absorber is depicted in Figure 1. A graphene layer is patterned on a grounded dielectric substrate. The substrate is chosen silicon dioxide, SiO_2 , which is applied for graphene structures [16]. A 0.5 μm thick gold layer is employed as ground plane. The thickness of gold should be more than the skin depth in terahertz frequencies to eliminate any transmission from the structure. Thus, considering zero transmission, absorption of the structure is defined as follows:

$$A = 1 - |S_{11}|^2 \quad (5)$$

where, S_{11} represents the reflected wave.

In this paper we have assumed a thickness of 1 nm for graphene sheet, which is reasonable [13]. Other parameters of graphene are shown in Table 1.

The unit cell of the metamaterial absorber, as shown in Figure 1(a), consists of four complementary square rings. The unit cell is designed on a complementary configuration in order to provide the possibility of applying graphene's bias voltage to the whole structure simultaneously. In this regard, four splits are applied on the rings to maintain continuity in graphene sheet.

TABLE 1. Parameters of graphene

Parameter	Value
thickness (nm)	1
temperature (K)	300
relaxation time (ps)	1
chemical potential (eV)	0-1

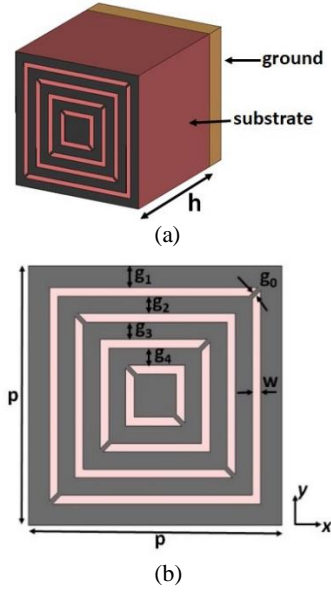


Figure 1. Unit cell of the absorber: (a) perspective, (b) top view

Design parameters of the structure including unit cell dimensions, square ring width and the gap between rings, are illustrated in Figure 1(b). Electric field of the incident wave is set along the y axis. Depending on the parameters, a dual-band absorber as well as an improved bandwidth absorber is designed and investigated. Numerical values of the two designs are shown in Table 2.

In order to investigate and explain the performance of the patterned graphene in the proposed absorber, an equivalent circuit model is developed. Since the graphene sheet is relatively ultra-thin compared to the wavelength (in THz regime), it can be considered as a shunt impedance in circuit model [18]. Figure 2 shows the mentioned equivalent circuit model, where $Z_0 = 120\pi \Omega$ is the free-space impedance, and Z_g and Z_d are the surface impedance of graphene and the impedance of SiO₂ dielectric, respectively. The gold layer is represented as a short circuit in the proposed equivalent circuit model.

TABLE 2. Parameters of the metamaterial absorber

Parameter	Dual-band	Improved bandwidth
h	5 μm	5 μm
p	3 μm	3 μm
w	0.05 μm	0.05 μm
g ₀	0.05 μm	0.05 μm
g ₁	0.025 μm	0.025 μm
g ₂	0.05 μm	0.1 μm
g ₃	0.05 μm	0.4 μm
g ₄	0.05 μm	0.05 μm
μ_c	0.5 eV	0.5 eV

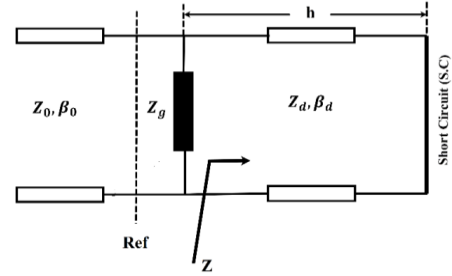


Figure 2. The equivalent circuit model of the absorber

Since the dielectric is lossless, the relative permittivity has only a real part ($\epsilon_d = 4.41$). Thus, the impedance of SiO₂ dielectric is $Z_d = Z_0/\sqrt{\epsilon_d}$ and the phase difference experienced by a signal traveling through this dielectric slab with a thickness h is defined as: $\phi_d = \beta_d h = 2\pi n_d h/\lambda_0$ where β_d , λ_0 and n_d are propagation constant, the free-space wavelength and refractive index of the dielectric, respectively.

Based on the proposed equivalent circuit model, we use transmission line theory to extract the impedance of graphene [18]. Therefore, the graphene sheet impinged by a plane wave normally and by using the finite difference frequency domain (FDFD) numerical method, the calculated reflection coefficient (S_{11}) at the reference plane; Ref is employed to obtain Z_g according to the following equation:

$$Z_g = \frac{Z_0 Z(1+S_{11})}{Z(1-S_{11}) - Z_0(1+S_{11})} \quad (6)$$

where, $Z = iZ_d \tan(\phi_d)$ is the input impedance of the dielectric slab as shown in Figure 2.

Figure 3 shows the results of the analytical solution. In this approach, the graphene chemical potential is varied between 0.5 and 1 eV and the distribution of the real and imaginary parts of Z_g calculated in the frequency range of the designed absorber are illustrated in Figures 3(a) and 3(b), respectively.

As can be observed from Figure 3, the maximum spectra shows a red shift for $Re(Z_g)$ and a blue shift for $Im(Z_g)$ as the chemical potential is decreased. Furthermore, as shown in Figure 3, by increasing the chemical potential, the lower values of graphene's impedance spectra is broadened. Moreover, Figure 3(b) also shows that there are frequency bands, over which $Im(Z_g) \leq 0$, implying capacitive impedance behavior for the graphene in the designed absorber.

4. SIMULATION RESULTS

Absorption of the dual-band design is plotted in Figure 4. Two 90% absorption at frequencies of 4.92 THz and 5.95 THz is observed, when graphene's chemical potential is set to 0.5 eV. The unit cell's lateral dimensions are

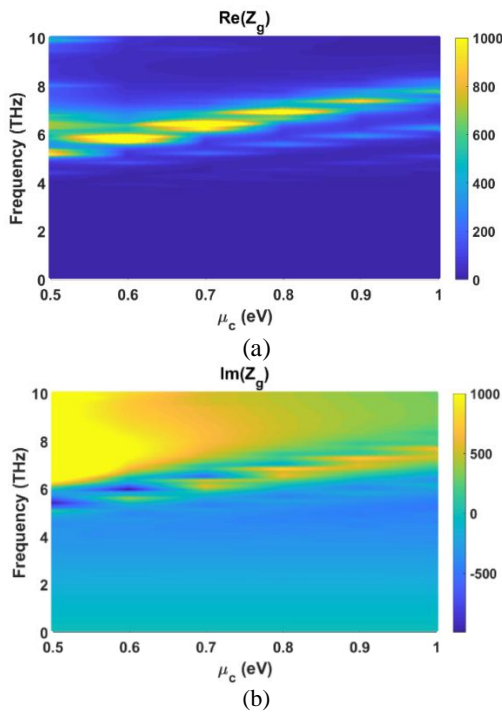


Figure 3. Distribution of the real part, (a) and the imaginary part, (b) of the graphene impedance (Ω) versus its chemical potential (horizontal axis) and the frequency range (vertical axis)

$0.049\lambda_0 \times 0.049\lambda_0$ at the lower resonant frequency, which is quite compact.

To better understand manipulation of light through plasmonic resonances, the magnitude of electric field at the resonant frequency of 4.92 THz is investigated and plotted in Figure 5. The electric field on graphene layer, xy plane, is depicted in Figure 5. As shown in the figure, electric field is concentrated along gaps of the complementary square rings due to formation of localized plasmonic resonances. Electric field on the unit cell's cross section, yz plane, is investigated and is shown in Figure 6. The field is plotted on two planes: $x=0$, center of unit cell, and $x=1.45$ mm, near the unit cell's edge beneath the gaps.

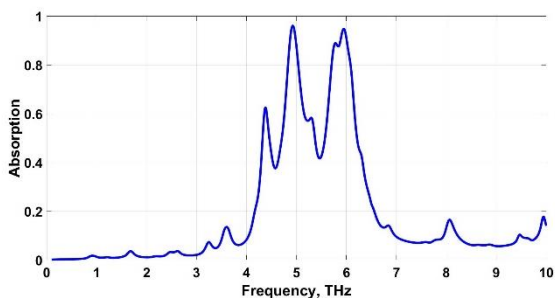


Figure 4. Absorption of dual band design

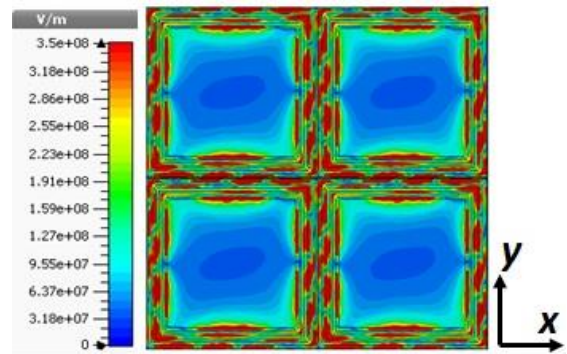


Figure 5. Magnitude of electric field at $f=4.92$ THz on graphene layer

It is observed that fields are concentrated under the gaps of the complementary rings, which is quite compatible with field plots on graphene surface shown in Figure 5. Graphene's chemical potential is varied and absorption of the structure is investigated and plotted in Figure 7. The figure demonstrates that with an increment of μ_c , frequencies of both absorption peaks increase and therefore a tunable dual band absorber is achieved.

Effects of incident and polarization angles on absorber performance is investigated and is plotted in Figure 8. With an increasing incident angle, absorption gradually

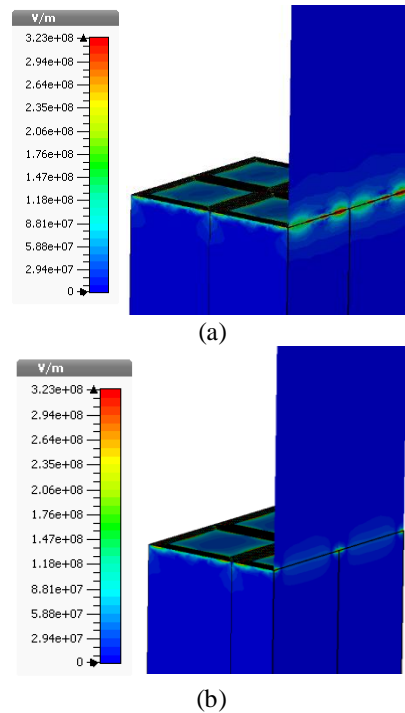


Figure 6. Magnitude of electric field at $f=4.92$ THz on unit cell cross section: (a) near the edge of unit cell, $x=1.45$ mm, (b) at the center of unit cell, $x=0$

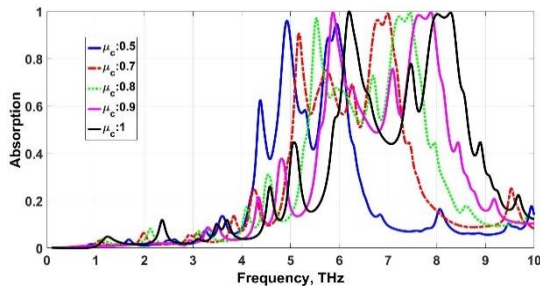
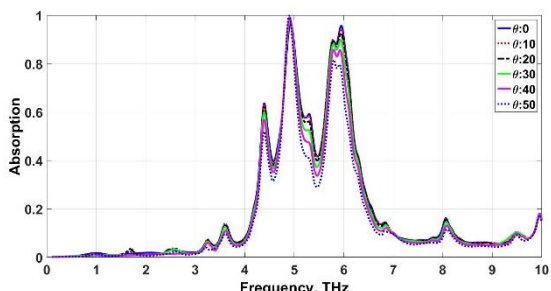


Figure 7. Absorption of dual-band design versus graphene's chemical potential

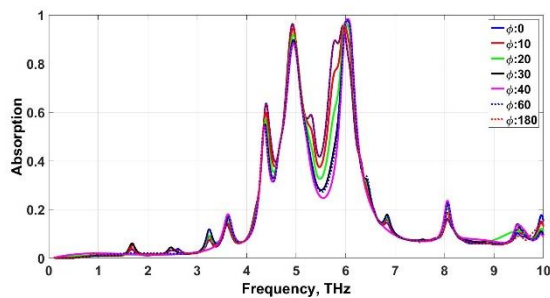
degrades and up to $\Theta=30^\circ$ dual band absorption peak exists, as shown in Figure 8(a). The increase of incident angle beyond 30 degrees, causes one of the absorption peaks to fall below 90%.

With increasing the polarization angle, absorption also degrades and dual band absorption is observed for incident angles up to 30 degrees. Because of symmetry of the structure, degradation occurs for polarization angle up to 45 degrees as well and beyond that improvement of absorption is observed. However, at polarization angle of 180 degrees the initial dual band behaviour is reached.

With varying parameters of the complementary rings, an absorber with improved bandwidth of 13.2%, for 90% absorption, is achieved. Parameters of the design are shown in Table 2 while absorption of the improved-bandwidth design is plotted in Figure 9. For this design, a dynamically tunable absorber is also achieved with changing graphene's chemical potential.



(a)



(b)

Figure 8. Effect of polarization and incident angle on absorption of dual-band design

Absorption of the structure with increasing μ_c is simulated and is demonstrated in Figure 10. It is illustrated that with small increments of graphene's chemical potential, absorption band moves toward higher frequencies. An improvement in absorption bandwidth, with increasing graphene's chemical potential, is also observed.

The absorber's performance with varying incident and polarization angles of the incoming wave is simulated and illustrated in Figure 11.

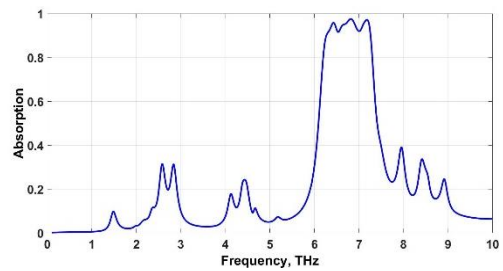


Figure 9. Absorption of the improved bandwidth design

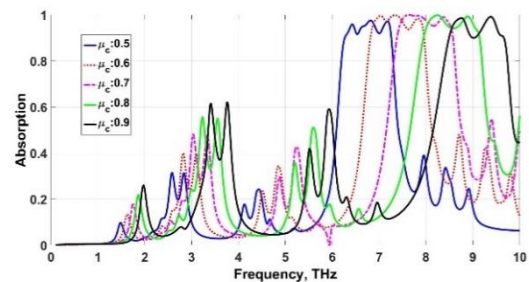
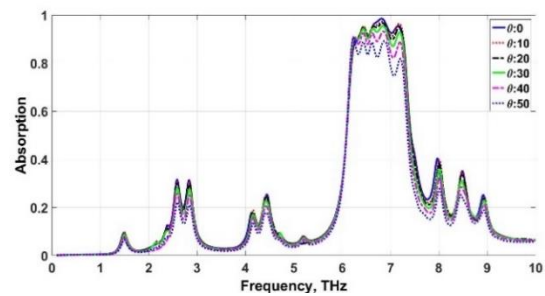
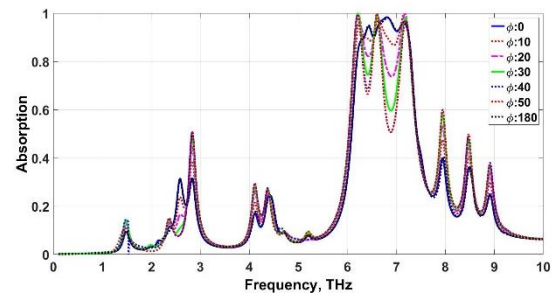


Figure 10. Absorption of the improved bandwidth design versus graphene's chemical potential



(a)



(b)

Figure 11. Effect of polarization and incident angle on absorption of improved-bandwidth design

As shown in Figure 11(a), wide band absorption is preserved until incident angle of 20 degrees, and further increase of incident angle results in reduction of bandwidth.

With increasing polarization angle, wide band performance transforms to tri-band absorption. This is compatible with the fact that, wide band performance is provided through three nearby resonances. Although with increasing ϕ in excess of 45 degrees improvement of absorption is occurred, for ϕ equal to 180 degrees the initial response is reproduced.

5. CONCLUSION

In this paper a tunable metamaterial absorber, in low Terahertz frequency band was designed and investigated. The structure was composed of 0.5 μm thick gold layer, as ground plane, which was covered by a layer of SiO_2 with 5 μm thickness, as substrate, and a patterned graphene sheet on the top. The proposed absorber was investigated theoretically and through simulations. Two sets of parameter values with identical unit cell dimensions were studied. The first design provided a dual band absorber with more than 90% absorption. The second design achieved improved bandwidth of 13.2% for 90% absorption. It was shown that both designs provided quite dynamically tunable structures with varying graphene's chemical potential. Electric field magnitude, on the surface of graphene layer as well as on the structure's cross section was studied thoroughly. Impact of incident and polarization angles on absorption performance of the two designs were studied and graphically demonstrated.

6. REFERENCES

- Caloz, C., "Dual composite right/left-handed (D-CRLH) transmission line metamaterial", *IEEE Microwave and Wireless Components Letters*, Vol. 16, No. 1, (2006), 585-587.
- Gil, M., Bonache, J., Garcia-Garcia, J., Martel, J., Martin, F., "Composite Right/Left-Handed Metamaterial Transmission Lines Based on Complementary Split-Rings Resonators and Their Applications to Very Wideband and Compact Filter Design", *IEEE Transactions on Microwave Theory and Techniques*, Vol. 55, No. 6, (2007), 1296-1304.
- Fakharian, M. and Rezaei, P., "Parametric study of uc-pbg structure in terms of simultaneous amc and ebg properties and its applications in proximity-coupled fractal patch antenna", *International Journal of Engineering, Transactions A: Basics*, Vol. 25, No. 4, (2012), 347-352.
- Jarchi, S., Rashed-Mohassel, J., Faraji-Dana, R. and Shahabadi, M., "Complementary periodic structures for miniaturization of planar antennas", *International Journal of Engineering, Transactions A: Basics*, Vol. 28, No. 10, (2015), 1463-1470.
- Jarchi, S., Soltan-Mohammadi, O., Rashed-Mohassel, J., "A planar, layered ultra-wideband Metamaterial absorber for microwave frequencies", *International Journal of Engineering, Transactions C: Aspects*, Vol. 30, No. 3, (2017), 338-343.
- Wang, B.X., Zhai, X., Wang, G.Z., Huang, W.Q., Wang L.L., "Design of a Four-Band and Polarization-Insensitive Terahertz Metamaterial Absorber", *IEEE Photonics Journal*, Vol. 7, No. 1, (2015), (4600108).
- He, X., Yan, S., Ma, Q., Zhang, Q., Jia, P., Wu, F., Jiang, J., "Broadband and polarization-insensitive terahertz absorber based on multilayer metamaterials", *Optics Communications*, Vol. 340, (2015), 44-49.
- Wang, B.X., Wang, L.L., Wang, G.Z., Huang, W.Q., Li, X.F., Zhai, X., "Metamaterial-Based Low-Conductivity Alloy Perfect Absorber", *Journal of Lightwave Technology*, Vol. 32, No. 12, (2014), 2293-2298.
- Cheng, Y., Nie, Y., Gong, R., "A polarization-insensitive and omnidirectional broadband terahertz metamaterial absorber based on coplanar multi-squares films", *Optics & Laser Technology*, Vol. 48, (2013), 415-421.
- Huang, L., Chowdhury, D.R., Ramani, S., Reiten, M.T., Luo, S.N., Azad, A.K., Taylor, A.J., Chen, H.T., "Impact of resonator geometry and its coupling with ground plane on ultrathin metamaterial perfect absorbers", *Applied Physics Letters*, Vol. 101, No. 10, (2012), <https://doi.org/10.1063/1.4749823>.
- Chen, H.T., O'Hara, J.F., Taylor, A.J., Averitt, R.D., "Complementary planar terahertz metamaterials", *Optics Express*, Vol. 15, No. 3, (2007), 1084-1095.
- Fan, Y., Wei, Z., Zhang, Z., Li, H., "Enhancing infrared extinction and absorption in a monolayer graphene sheet by harvesting the electric dipolar mode of split ring resonators", *Optics Letters*, Vol. 38, No. 24, (2013), 5410-5413.
- Alaee, R., Farhat, M., Rockstuhl, C., Lederer, F., "A perfect absorber made of a graphene micro-ribbon metamaterial", *Optics Express*, Vol. 20, No. 27, (2012), 28017-28024.
- Khavasi, A., "Design of ultra-broadband graphene absorber using circuit theory", *Journal of the Optical Society of America B*, Vol. 32, No. 9, (2015), 1941-1946.
- Andryieuski, A., Lavrinenko, A.V., "Graphene metamaterials based tunable terahertz absorber: effective surface conductivity approach", *Optics Express*, Vol. 21, No. 7, (2013), 9144-9155.
- Yao, G., Ling, F., Yue, J., Luo, C., Luo, Q., Yao, J., "Dynamically Electrically Tunable Broadband Absorber Based on Graphene Analog of Electromagnetically Induced Transparency", *IEEE Photonics Journal*, Vol. 8, No. 1, (2016), <https://doi.org/10.1109/JPHOT.2015.2513210>.
- Grigorenko, A.N., Polini, M., Novoselov, K.S., "Graphene plasmonics", *Nature Photonics*, Vol. 6, (2012), 749-758.
- Gómez-Díaz, J.S., Perruisseau-Carrier, J., Sharma, P., Ionescu, A., "Non-contact characterization of graphene surface impedance at micro and millimeter waves", *Journal of Applied Physics*, Vol. 111, No. 11, (2012).

Dual-band, Dynamically Tunable Plasmonic Metamaterial Absorbers Based on Graphene for Terahertz Frequencies

S. Jarchi^a, J. Rashed-Mohassel^b, M. Mehranpour^a

^a Faculty of Technical and Engineering, Imam Khomeini International University (IKIU), Qazvin, Iran

^b School of Electrical & Computer Engineering, College of Engineering, University of Tehran, Tehran, Iran

P A P E R I N F O

چکیده

Paper history:

Received 23 May 2018

Received in revised form 19 January 2019

Accepted 07 March 2019

Keywords:

Graphene

Metamaterial

Terahertz Absorber

Tunable Absorber

Dual-band Absorber

در این مقاله یک جاذب فراماده پلاسمونی فشرده برای فرکانسهای تراهرتز پیشنهاد شده و شبیه سازی شده است. جاذب براساس ساختارهای گرافنی فراماده می باشد و از ویژگی قابلیت کنترل پویای گرافن بهره می برد. با استفاده از شکل دهی لایه گرافن، تشدیدهای پلاسمونی طوری طراحی شده اند که جذب دو باند، و همین طور جذب با پهنای باند بهبود یافته بدست آید. سلول واحد ساختار طراحی شده از چهار حلقه مربعی مکمل تشکیل شده است که روی یک لایه SiO_2 زمین شده با ضخامت ۵ میکرومتر قرار دارند. در حلقه های مربعی چهار شکاف قرار داده شده است تا پیوستگی لایه گرافن حفظ شود. جذب دو باند بالای ۹۰٪ بدست آمده است، به طوری که فرکانس بیشینه جذب با افزایش پتانسیل شیمیایی گرافن زیاد می شود. نشان داده شده است که با تغییر ابعاد حلقه های شکاف دار، جاذب با پهنای باند بهبود یافته محقق می شود که در آن نیز باند جذب با افزایش پتانسیل شیمیایی گرافن افزایش می یابد. به منظور درک بهتر برانگیختگی تشدیدهای پلاسمونی در ساختار پیشنهاد شده، گسترده گی میدان الکتریکی روی لایه گرافن، و همین طور در سطح برش سلول واحد بررسی شده و با استفاده از شکل نشان داده شده است. وابستگی جذب به زوایای تابش و قطبش موج برخوردی مطالعه و ارایه شده است.

doi: 10.5829/ije.2019.32.4a.07